

# First Detection of Low-Energy Electrons with Transition Edge Sensors

Carlo Pepe,<sup>1</sup> Benedetta Corcione,<sup>2,3</sup> Francesco Pandolfi,<sup>3,\*</sup> Hobey Garrone,<sup>1</sup> Eugenio Monticone,<sup>1</sup> Ilaria Rago,<sup>3</sup> Gianluca Cavoto,<sup>2,3</sup> Alice Apponi,<sup>4</sup> and Mauro Rajteri<sup>1</sup>

<sup>1</sup>*Istituto Nazionale di Ricerca Metrologica, Strada delle Cacce 91, 10135 Torino*

<sup>2</sup>*Sapienza Università di Roma, Piazzale Aldo Moro 2, 00185 Rome, Italy*

<sup>3</sup>*Istituto Nazionale di Fisica Nucleare - Sezione di Roma, Piazzale Aldo Moro 2, 00185 Rome, Italy*

<sup>4</sup>*Dipartimento di Scienze Università degli Studi Roma Tre,*

*and Istituto Nazionale di Fisica Nucleare - Sezione di Roma Tre, Via della Vasca Navale 84, 00146 Rome, Italy*

We present the first detection of electrons with kinetic energy in the 100 eV range with transition edge sensors (TES). This has been achieved with a  $100 \times 100 \mu\text{m}^2$  Ti-Au bilayer TES, with a critical temperature of about 83 mK. The electrons are produced by a cold cathode source based on field emission from vertically-aligned multiwall carbon nanotubes. The obtained energy resolution is smaller than 2 eV for fully-contained electrons, while significant non-containment is observed. This measurement opens new possibilities in the field of electron detection, and constitutes the first detection of such particles without any form of particle multiplication.

Transition edge sensors (TES) are highly sensitive micro-calorimeters capable of high-resolution single-photon counting across a wide energy spectrum. The detection scheme is based on the absorption of the incoming photons in a thin superconducting film, in which their energy is transformed into heat. By operating a TES device at its critical temperature  $T_C$ , even small variations in temperature lead to measurable changes in its electrical resistance, owing to the steep transition between the superconducting regime and the normal-conduction one. TES devices have been capable of achieving single-photon energy resolutions, defined throughout this work as the standard deviation of the distribution, as low as  $\sigma = 0. X \text{ eV}$  [1]. In principle, this detection scheme should also be sensitive to electrons absorbed in the superconducting film, yet there is very little research on TES devices used in electron detection. The use of TES devices in electron detection could be of great interest to a vast number of experiments, such as, for example, the PTOLEMY collaboration [2], which plans to search for the cosmic neutrino background by analyzing the endpoint of the beta decay of tritium with unprecedented electron energy resolution.

The results presented in this work were obtained in the innovative cryogenic detectors laboratory of the photometry division of Istituto Nazionale di Ricerca Metrologica (INRiM) in Torino. The TES detectors operate on the 30 mK stage of a commercial pulse-tube driven adiabatic demagnetization refrigerator cryostat (Model 103-RC Rainier from HPD [3]). The TES device used in this work has a size of  $100 \times 100 \mu\text{m}^2$ , and is a Ti-Au bilayer device, composed by 15 nm of titanium covered by 30 nm of gold, fabricated at INRiM by thermal evaporation on a 500 nm silicon nitride substrate [3]. It is wired with 50 nm superconducting niobium (Nb) traces, which were deposited on the substrate via sputtering. The TES has a critical temperature  $T_C = 84 \text{ mK}$  and was calibrated with 406 nm photons, obtaining an energy resolution between 0.7 and 1.2 eV in the 0 – 100 eV energy range.

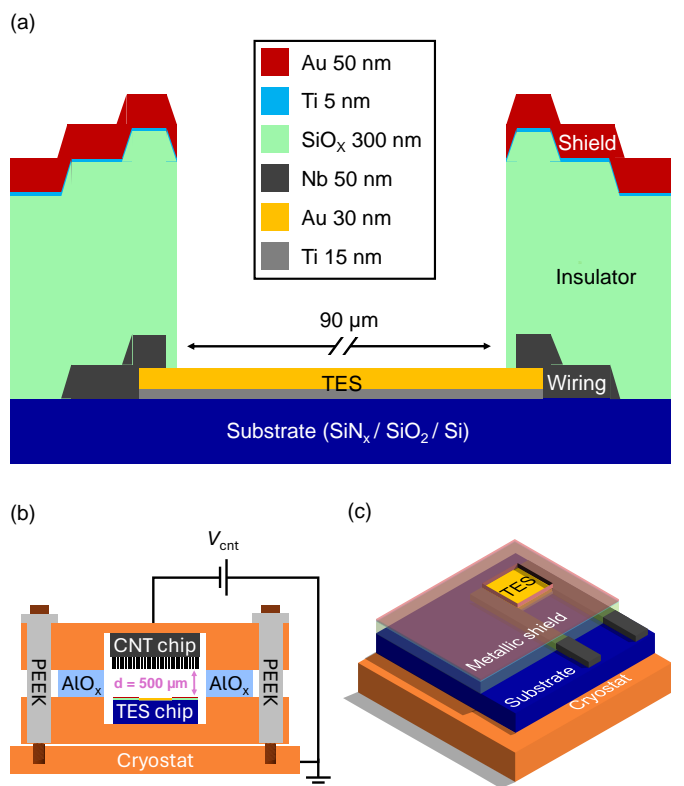


FIG. 1. Top: schematic view of the TES device and its shielding layer (image is not to scale). Bottom: schematic view of the setup use for electron counting: the carbon nanotubes (CNTs) are hosted on the top copper plate and oriented with the tips pointing towards the TES.

This design was adapted for electron detection by adding a shield layer, which is needed as the electron source has a significantly larger area (approximately  $1 \times 1 \text{ mm}^2$ ) compared to the TES active area ( $100 \times 100 \mu\text{m}^2$ ). Therefore it is necessary to avoid direct electron hits on the Nb wiring, which would induce electric noise, and

also to cover the surface of the substrate surrounding the TES, which is insulating at cryogenic temperatures and therefore exposing it to a direct electron current would lead to charge build-up. The shield layer is produced by first depositing an insulating layer consisting of 300 nm of silicon oxide ( $\text{SiO}_x$ ), followed by a thin (5 nm) layer of titanium, and finally a 50 nm layer of gold. The thin titanium layer is necessary for best adhesion to the  $\text{SiO}_x$ . A schematic view of the detector and the shield layer is shown in the top panel of Figure 1.

The electron source consists of a sample of vertically-aligned multi-wall carbon nanotubes which were synthesized in the INFN laboratory ‘TITAN’ at Sapienza University of Rome. The nanotubes were grown through chemical vapor deposition on a 500  $\mu\text{m}$  silicon substrate, and are approximately 200 microns in length, while covering a surface of roughly  $1 \times 1 \text{ mm}^2$ . Thanks to the high geometrical field enhancement factor of their tips, nanotubes are capable of emitting electrons through quantum tunneling (field emission) without the necessity of applying very high voltages. Furthermore, as this emission is quantic in nature, and not thermal, it does not generate heat and can therefore be used in a cryostat.

The TES and the nanotubes were placed on two copper plates, facing each other, separated by 0.5 mm sapphire spacers, which ensure electrical insulation while guaranteeing a good degree of thermal conductance. The top copper plate, where the nanotubes are hosted, was connected to the power supply of a Keithley 6487, and was provided negative voltage  $V_{\text{cnt}}$  in order to produce field-emission electrons; the bottom plate was put in thermal contact with the cryostat, and grounded electrically through it. The distance between the tips of the nanotubes and the surface of the TES, in this setup, is  $d = 0.5 \text{ mm}$ . A schematic view of the setup is shown in the bottom panel of Figure 1.

The TES was read-out in two different ways. In the ‘anode’ configuration it is short-circuited to the metallic layer of the shield layer, and the two are used as a large-area metallic plate which is in turn connected to the Keithley 6487 picoammeter to measure the current  $I_{\text{cnt}}$  emitted by the nanotubes. In the ‘counting’ configuration the TES is sensitive to single-particle signals. This is achieved by bringing the TES to a temperature equal to  $T_C$  by circulating a current  $I_{\text{tes}}$  through it until it reaches its nominal working point, defined as the TES having a resistance  $R_{\text{tes}} = 0.35 \cdot R_N$ , where  $R_N$  is the resistance of the TES in normal mode. The TES is then read out with a DC-SQUID transimpedance amplifier. In counting mode the metallic shield is grounded through the cryostat.

The results in the anode configuration are summarized in the black curve of Figure 2, where  $I_{\text{cnt}}$  is shown as a function of  $V_{\text{cnt}}$ . As can be seen,  $I_{\text{cnt}}$  exhibits an exponential rise, compatibly with the Fowler-Nordheim theory on field emission [6]. Superimposed on the same plot

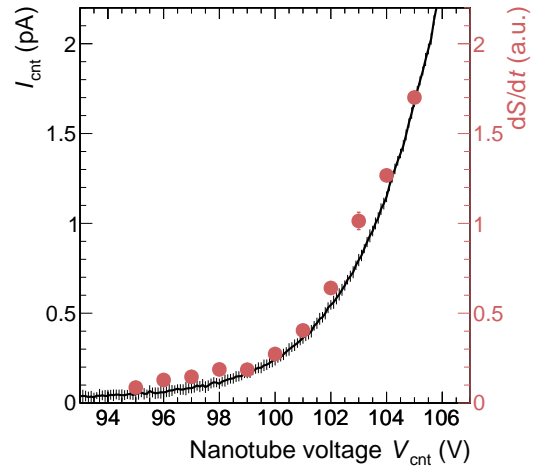


FIG. 2. Current  $I_{\text{cnt}}$  emitted by the nanotube source (black curve, right vertical scale), as a function of the negative voltage  $V_{\text{cnt}}$  provided to it, when reading the TES and the shield in anode configuration, compared to the rate of signals  $dS/dt$  (cyan markers, left vertical scale) recorded by the TES read-out in counting configuration.

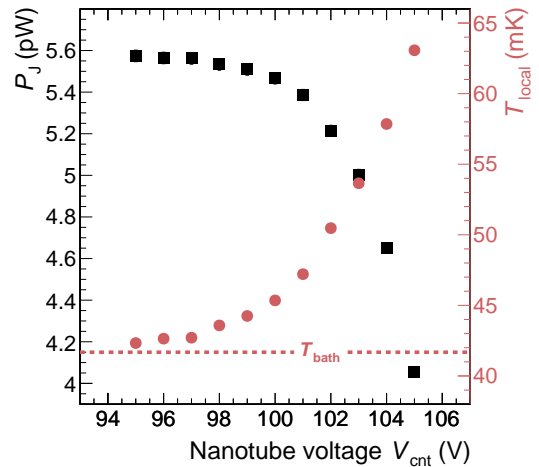


FIG. 3. Power needed to bring the TES to its critical temperature (black markers, left vertical scale) and local temperature of the substrate under the TES device (red markers, right vertical scale) for different values of  $V_{\text{cnt}}$ . The bath temperature is marked with a dashed line.

with cyan markers is the rate of signals  $dS/dt$  measured with the TES in counting mode. As can be seen the increase in  $dS/dt$  as a function of  $V_{\text{cnt}}$  follows the same exponential rise as that of  $I_{\text{cnt}}$ , therefore proving that the signals recorded by the TES are due to electrons.

A feature of Fowler-Nordheim emission is that the current of emitted electrons by the nanotubes depends on the electric field  $|\vec{E}|$  in proximity of their tips, which in our planar configuration corresponds, in first approxima-

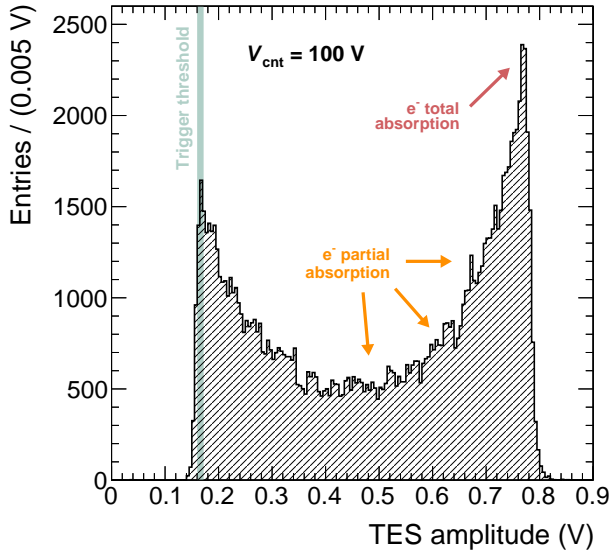


FIG. 4. Typical spectrum of TES signal amplitudes. This spectrum was obtained with  $V_{\text{cnt}} = 100$  V.

tion, to  $|\vec{E}| = V_{\text{cnt}}/d$ . At the same time, if we assume that electrons are emitted by the nanotubes with a null initial kinetic energy,  $V_{\text{cnt}}$  also determines the kinetic energy of the electrons when entering the TES. Therefore in this setup the signal rate and electron energy are not independent parameters, as they both depend on  $V_{\text{cnt}}$ .

As the electrons are emitted by a relatively large area compared to the TES, when  $V_{\text{cnt}}$  is raised the high rate of electrons hitting the TES and its surroundings produces heat. This means that to bring the TES to its nominal working point a smaller  $I_{\text{tes}}$  is needed, as its temperature is higher to begin with. This is shown in Figure 3, where the black markers, which represent the power needed to bring the TES to its nominal working point, can be seen clearly decreasing as  $V_{\text{cnt}}$  increases. This dissipated power can in turn be interpreted as the local temperature of the substrate in direct contact with the TES, which is graphed with blue markers in Figure 3: as can be seen, when operating the electron source at  $V_{\text{cnt}} = 105$  V the local temperature of the substrate is already higher than 60 mK, compared to the initial temperature of about 41 mK before electron emission. This implies that results at different  $V_{\text{cnt}}$  are not rigorously comparable, as the TES is operating in slightly different conditions.

For each value of  $V_{\text{cnt}}$ , the amplitude of the signals produced by the TES were analyzed. A typical spectrum, obtained for  $V_{\text{cnt}} = 100$  V is shown in Figure 4: as can be seen the distribution presents a high-amplitude peak, corresponding to the full absorption of the electron energy in the sensitive layer of the TES; a marked tail to the left of the peak, due to partial absorption of electrons, and is most likely due to longitudinal non-containment,

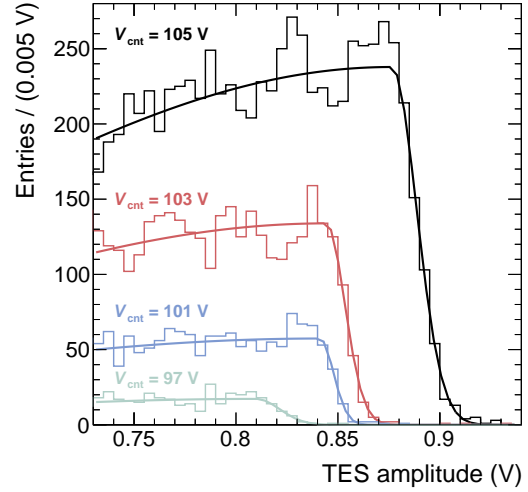


FIG. 5. Example fits, for four different values of  $V_{\text{cnt}}$ , of the high-amplitude peak with the asymmetric Gaussian function.

as the TES has a very thin gold layer (30 nm); and a low-amplitude peak, which is truncated by the trigger threshold of 166 mV.

We fit the distributions with an asymmetric Gaussian function, described by its peak position  $\mu$  and its left ( $\sigma_L$ ) and right ( $\sigma_R$ ) tails. Some example fits are shown in Figure 5.

The trend of the fitted value of  $\mu$  is shown in the left panel of Figure 6 shows the fitted values of  $\mu$ , as a function of the nominal energy  $E_e$  of the electrons, taken as  $E_e = V_{\text{cnt}} \cdot \frac{C}{e}$ , where  $C$  is the Coulomb charge and  $e$  is the charge of the electron. When operating the TES in the same conditions, the position of the absorption peak  $\mu$  should increase linearly with the energy of the absorbed electrons, therefore  $\mu \propto V_{\text{cnt}}$ . However, as explained previously, the working conditions of the TES were not exactly the same for each value of  $V_{\text{cnt}}$ , therefore some deviations from the linear trend are expected. Nevertheless, we observe a significant rise of the absorption peak position  $\mu$ .

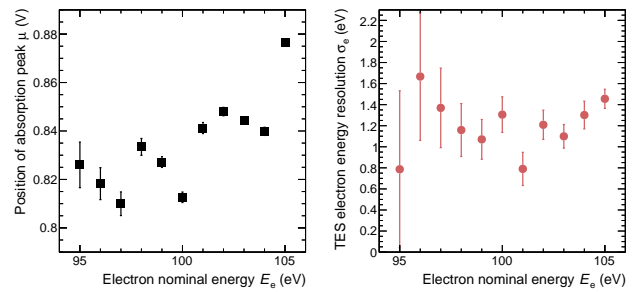


FIG. 6. Fitted position of the absorption peak  $\mu$  (left) and TES electron energy resolution  $\sigma_e$  (right) as a function of the nominal electron energy  $E_e$ .

Finally, the left panel of Figure 6 shows the trend of  $\sigma_e = (\sigma_R/\mu) \cdot E_e$  as a function of  $E_e$ . The parameter  $\sigma_R$  describes the broadness of the high-energy tail of the absorption peak in the amplitude distribution. While the left tail is dominated by electron non-containment effects, the right tail is dominated by the energy resolution of the device, plus possible small effects due to the non-monochromaticity of the source. When rescaling  $\sigma_R$  to the nominal energy  $E_e$  we obtain  $0.8 < \sigma_e < 1.8$  eV for all

values of  $E_e$ , and this can be interpreted as an estimate of the absolute energy resolution of the TES device when detecting electrons in the 100 eV energy range.

#### AGGIUNGERE LE CONCLUSIONI

---

\* francesco.pandolfi@roma1.infn.it